arXiv:1207.2068v1 [cond-mat.supr-con] 9 Jul 2012

Multifractal scaling of flux penetration in the Iron-based Superconductor $\mathbf{Ba(Fe_{0.925}Co_{0.075})_2As_2}$

Mathieu Grisolia and Cornelis J. van der Beek
Laboratoire des Solides Irradiés, CNRS UMR 7642 & CEA-DSM-IRAMIS,
Ecole Polytechnique, F91128 Palaiseau cedex, France

Anne Forget, Dorothée Colson
Service de Physique de l'Etat Condensé, Orme des Merisiers,
CEA Saclay (CNRS URA 2464), 91191 Gif sur Yvette cedex, France

(Dated: July 10, 2012)

The penetration of magnetic flux fronts in the optimally doped iron based superconductor $Ba(Fe_{0.925}Co_{0.075})_2As_2$ is studied by means of high resolution magneto-optic imaging. The analysis of roughening and growth of the magnetic flux front reveals anomalous scaling properties. While higher-order spatial correlation functions reveal multifractal behavior for the roughening, the usual Kardar-Parisi-Zhang growth exponent is found. Both exponents are found to independent of temperature. We propose a scenario for vortex penetration based on 2D percolation and cluster aggregation in an inhomogeneously disordered superconductor.

PACS numbers: 74.25.Wx,68.35.Ct,64.60.al,74.25.Op

I. INTRODUCTION

The magnetization properties of type-II superconductors have been studied for many years. The magnetization is usually described in terms of the Bean model and its generalizations. While the Bean model explains the global magnetization properties such as hysteresis loops, it does not describe the local fluctuations of vortex densities $n_v = |\mathbf{B}|/\phi_0$ in time and space,[1,2] that lead to intermittence in flux line motion, nor the roughness of the penetration magnetic flux front ($\mathbf{B}$ is the averaged or coarse-grained flux density and $\Phi_0 = h/2e$ is the flux quantum). Because of the wide range of phenomena in which front growth and roughening occur, such as fluid flow in porous media,[3] propagation of the ignition front in burning paper[1,4], or the advancement of a rice pile[5], and the many analogies between these different phenomena, the subject has raised a huge amount of interest over the last 25 years.

The analysis of local variations of the magnetic flux front height $h(x)$ is commonly performed using the height-height correlation function[6]

$$C^2(x,t) = < [h(x,t) - h(x+x', t+\tau)]^2 >_{x',\tau}, \qquad (1)$$

where $< \ldots >_{x,t}$ denotes averaging over the spatial coordinate as well as time; on our case, time steps will correspond to increments in the applied magnetic field $\mu_0 H_a$. This quantity enables one to simultaneously determine both the roughness exponent α and the growth exponent β by fitting the respective evolution

$$C(x,0) \propto x^{\alpha} \qquad (x \ll l_{sat}) \qquad (2)$$

$$C(0,t) \propto t^{\beta} \qquad (t \ll t_{sat}). \qquad (3)$$

The saturation length l_{sat} and saturation time t_{sat} are the length and time scales below which the evolution of different sites on the front depends on the heights of neighboring sites. The interaction with the front shape and evolution at neighboring sites will cause thus the front height fluctuations to spread laterally (roughness) and perpendicularly (growth).

Theoretical models predict very different scaling properties of interface roughening, as a function of its (non)equilibrium state and the type of disorder. These models usually describe the competition between two antagonistic mechanisms, such as the elasticity of the interface, which tends to smooth it, and its interaction with a disorder potential, responsible for roughening. A powerful theoretical approach to kinetic roughening is represented by the so-called Kardar-Parisi-Zhang (KPZ) equation[7] which describes the temporal development of the height variable $h(x,t)$,

$$\frac{\partial h}{\partial t} = \nu \nabla^2 h + \lambda (\nabla h)^2 + \eta. \qquad (4)$$

Here ν is an effective surface tension and λ quantifies the importance of lateral growth. Eq. (4) well describes diverse models of kinetic roughening such as ballistic deposition or Eden models[7] but also the advancement of flux fronts in type II superconductors[1]. This is because the growth of the flux front height is, through the action of the Lorentz force $\mathbf{F}_L = \mathbf{j} \times \mathbf{B}$, necessarily perpendicular to the front itself. The KPZ model predicts well-defined roughness and growth exponents, $\alpha = \frac{1}{2}$ and $\beta = \frac{1}{3}$. In parallel, however, a wide variety of exponents has been reported in other systems, including wetting, imbibition, percolation, bacteria invasion, and so forth.[8,9] Among different approaches to account for such phenomena, Barabási *et al.* proposed to apply the concept of multifractality to interface roughness.[10] Multifractality has been associated with a power-law distribution of the noise amplitude η, that accounts for rare events in the roughening or growing process. Also, it is relevant for the roughening of linear polymers on percolation clusters.[11–13] A multifractal formalism may be equally useful if different length scales compete in the growth process, or if depinning occurs at preferential sites. In those cases, rare events such as avalanches may drive the kinetic properties.[14,15]

Returning to magnetic flux fronts in superconductors, Surdeanu *et al*[1] were the first to study different models to account for the roughening of the interface between the Shubnikov and Meissner phase in thin–film cuprate superconductors. The authors[1] distinguished two regimes in roughening and growth: a short–range interaction regime was governed by the Directed Percolation Depinning (DPD) model[9], conceived for the imbibition of paper by a liquid[16], while the long–range regime is described by a usual 1+1-KPZ equation. Vlasko-Vlasov *et al.*[17] also reported DPD-like behavior ($\alpha = 0.63$) in a narrow temperature window, between smooth flux fronts at high T, and an avalanche-dominated regime at low T; however, they noted that the observed scaling might be due to KPZ behavior in the presence of spatially correlated (non-Gaussian) disorder.

The past four years have seen an exceptional interest for high–T_c iron–based superconductors.[18] In those unwonted and not yet fully understood superconductors, disorder leads to highly disordered equilibrium vortex structures. In Ref. 19, Demirdiş *et al.* suggested that crystalline disorder in $\mathrm{Ba(Fe_{0.925}Co_{0.075})_2As_2}$ is inhomogeneous, and that this heterogeneity leads to the total lack of positional order, as well as to the vortex density fluctuations observed on field cooling. It is quite possible that the presence of such heterogeneous material properties of the superconductor leads to non-Gaussian disorder correlators, and therefore, non-KPZ behavior. Alternatively, the interpretation of the results[19] in terms of variations of superconducting parameters such as the critical temperature T_c or the superfluid density, resulting in a random network of favorable and less favorable sites, imposes the analogy with front progression on a percolation cluster. We have therefore characterized the scaling properties of the penetrating flux front in single crystals of the optimally doped $\mathrm{Ba(Fe_{0.925}Co_{0.075})_2As_2}$ iron-based superconductor, not only following the method proposed by Surdeanu *et al.*, but extended to the recently developed multiscaling approach. Multi-fractal behavior is observed for the roughness exponent, while the growth exponent remains in agreement with KPZ theory.

II. EXPERIMENTAL DETAILS

Single crystals of $\mathrm{Ba(Fe_{1-x}Co_x)_2As_2}$ have been grown using the self-flux method as described in Ref. 20. We have measured and analyzed magnetic flux penetration fronts in single crystals of the optimally doped superconducting composition $\mathrm{Ba(Fe_{0.925}Co_{0.075})_2As_2}$. Crystal # 1 has a length of 994 μm, a width of 571 μm, and a thickness of 32 μm, and a critical current density (at $T = 10$ K) $j_c = 2.4 \times 10^8\,\mathrm{Am^{-2}}$; crystal # 2 has a length of 835 μm, a width of 733 μm, a thickness of 27 μm, and $j_c(10\,\mathrm{K}) = 3.1 \times 10^8\,\mathrm{Am^{-2}}$.

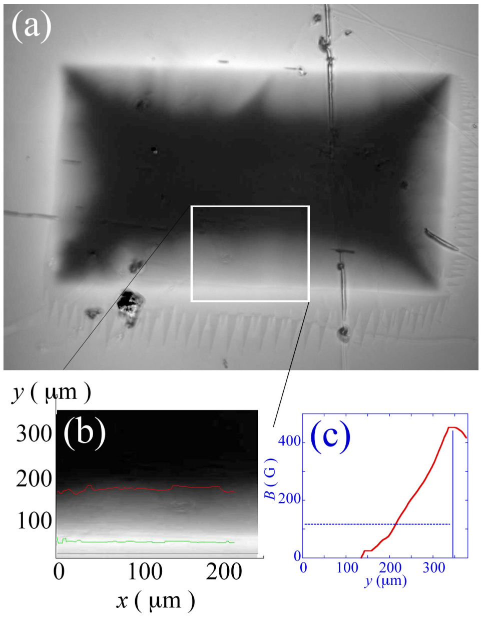

FIG. 1: (a) MO image of flux-penetration into $\mathrm{Ba(Fe_{0.925},Co_{0.075})_2As_2}$ crystal # 1, taken at $H_a = 404$ G after zero field cooling to 10 K. The zoom in (b) shows the part that is used in the analysis. The red line indicates the flux front, determined as the induction threshold $B = 12$ mT above the luminous intensity value corresponding to the Meissner state. The green line shows the crystal edge. (c) Average Bean–like flux density profile along the y-direction in the region magnified in (b).

The penetration of magnetic flux into the selected crystals, was visualized by the magneto-optical imaging (MOI) method.[21,22] A ferromagnetic garnet indicator film with in-plane anisotropy is placed on top of the sample, and a polarized light microscope is used to observe it. The Faraday rotation of the light traversing the indicator allows for the detection of regions with nonzero perpendicular component of the magnetic flux density B, which show up as bright when observed through an analyzing polarizer, see Fig. 1. Regions of non-zero B correspond to the applied field outside the crystal boundaries, and to the Shubnikov phase (within the crystal boundaries). Dark regions correspond to $B = 0$ (Meissner Phase). In order to avoid bias and distortions induced by the effect of the crystal corners on the shape of the flux fronts, we studied the penetration near the center of the crystal edges only.

The MO images are converted to maps of the magnetic induction by calibration of the luminous intensity with respect to the applied field.[22] Next, the position of the flux front is determined from a threshold level of 120 G of the magnetic induction on the flux profiles. This is to avoid uncontrolled variations between experiments due to the specific luminosity and polarization conditions under

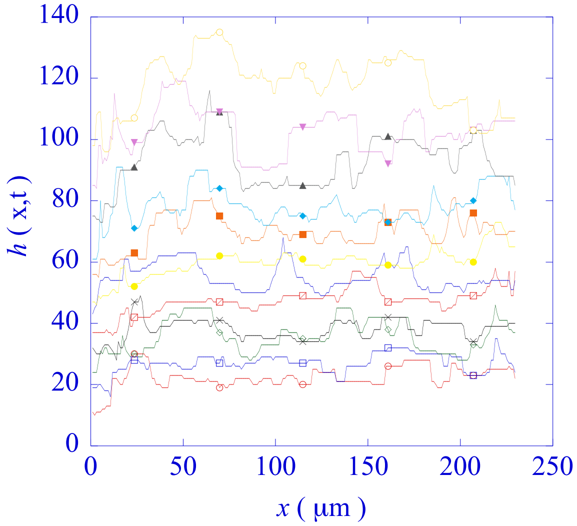

FIG. 2: Flux fronts observed in crystal # 1 at 10 K. The value of the external applied field ranges from 163 G (bottom) to 383 G (top).

which images are acquired. we define the height of the flux front as the distance between the position at which the magnetic induction is maximum at the sample boundary, and the position of this intensity threshold, along a 1 pixel-wide strip perpendicular to the image boundary. Such a definition eliminates the effect of possible shifts in the luminous intensity due to over-exposure of certain strips in the CCD. Specific care was taken for the monitoring of the flux front's progression. The temperature was stabilized to less than 10 mK, and the external field was increased in 20 Oe steps.

The correlation function defined in Eq. (1) is sensitive to bias in the data, *i.e.*, if the interface has an overall slope, the scaling is affected. In experimental data, even if every precaution was taken during experimental acquisition, there may still remain a slope. To overcome this effect we define a slightly different height variable $\delta h(x,t) = h(x,t) - \langle h(t) \rangle_x$. Thus we compute the two-point correlation function on the variable δh instead of h. An example of the progression of the flux front so determined in crystal # 1 is shown in Fig. 2.

III. ANALYSIS OF THE MAGNETIC FLUX FRONT

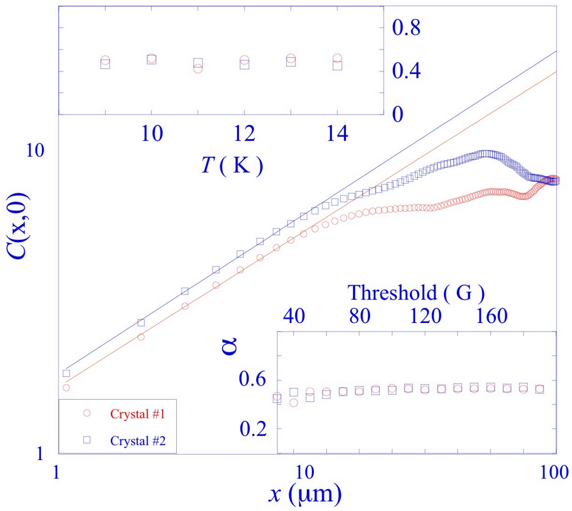

FIG. 3: Main panel : Two-point correlation function of the penetrating flux front, calculated according to Eq. (1) in crystal # 1(red) and # 2 (blue), at 10 K. The roughness exponent is, by definition, the slope of the linear (solid lines) regime of $C(x,0)$ in a log-log plot. For crystal # 2, this value is in perfect agreement with KPZ, *i.e.* $\alpha = 0.50$. Upper inset: Temperature independence of the roughness exponent – α remains around the value of 0.5. Lower Inset: Independence of α as a function of the threshold value of the magnetic induction B, as this ranges from 4 to 20 mT.

Figure 3 shows the spatial correlation function $C(x,0)$. The value of the roughness exponent, $\alpha \sim 0.5$, determined from the logarithmic slope of $C(x,0)$ versus x, is very close to the value derived from the KPZ model.[6] In this respect, our data are similar to those of Surdeanu *et al.*.[1] In order to ascertain the robustness of our results, we have checked for temperature and vortex density dependence. At low flux densities, the distance between vortex lines, $a_0 = n_v^{-1/2}$, exceeds the penetration depth $\lambda_L(T)$; for given B, the repulsive interaction between vortices then increases with T. At higher flux densities, $a_0 < \lambda_L(T)$, and the repulsive interaction decreases with T. Hence, vortex lines may not be sensitive to disorder on the same length scale for different T and n_v. The dependence on vortex density amounts to changing the threshold level used for the determination of the front height. The upper inset to Fig. 3 shows, however, that the roughness exponent does not clearly depend on temperature. This seems to be contrary to observations on superconducting Nb by Vlasko-Vlasov *et al.*,[17] in which very different temperature regimes of penetration were observed. The lack of any dependence of the front roughness on the strength of the vortex interaction is underscored by the independence of α on the threshold value of B, displayed in the lower inset to Fig. 3. A tentative explanation is suggested by Ref. 19, namely that the Ba(Fe$_{1-x}$,Co$_x$)$_2$As$_2$ crystals are disordered on widely different length scales, so that vortex lines always find an optimally pinned site.

We now turn to the multiscaling analysis of the data. The method is straight-forward.[12,29] It relies on the computation of the multiple-order two–point correlation function

$$C_q(x,t) = \langle [\delta h(x,t) - \delta h\,(x+x',t+\tau)]^q \rangle_{x',\tau}{}^{1/q}. \quad (5)$$

Following previous work, C_q should scale as $C_q(x,0) \propto$

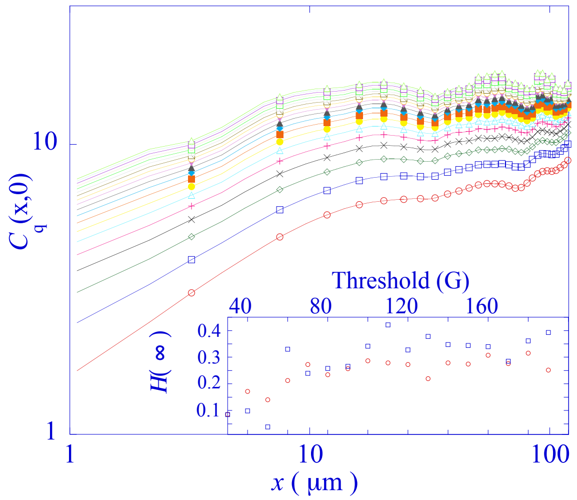

FIG. 4: Higher order spatial correlation function $C_q(x,t)$, with q varying from 2 to 20, as measured on the penetrating flux front in $Ba(Fe_{0.925}Co_{0.075})_2As_2$ crystal # 2 at $T = 10$ K. The slope depends continuously on q and presents nontrivial scaling. The behavior is therefore multifractal. The same behavior is found for sample #1.

x^{qH_q},[10] with H_q the generalized Hurst exponent. A nontrivial q-dependent scaling is the hallmark of multifractal behaviour, *i.e* the geometry of the interface is not simply fractal but implies many different geometries of many different fractal dimensions. A constant $\alpha = 0.5$ is the hallmark of KPZ behavior (see Ref. 10 and Fig. 5). Figure 4 shows the higher order two-point correlation functions evaluated on the flux fronts in crystal # 1. Here q ranges from 2 to 20. Clearly, the scaling with length depends on the order q. Figure 5 shows the behavior of the exponent H_q as a function of q for the magnetic flux fronts in our $Ba(Fe_{0.925},Co_{0.075})_2As_2$ crystals. The saturation of H_q to a value of ~ 0.3 at large q is the result of the resolution limit in our experiment.

We have also evaluated multiscaling of growth of the flux front height. Figure 6 shows that the temporal correlation functions $C_q(0,t) = C_q(0, H_a/\dot{H}_a)$ are parallel for all q, obeying $C_q(0,t) \sim t^{0.21}$ at small t (small H_a). We consider this small value to be in agreement with $\beta = \frac{1}{3}$ from KPZ theory. We thus find, surprisingly, that the evolution of the flux fronts in the $Ba(Fe_{0.925}Co_{0.075})_2As_2$ crystals corresponds to the diffusive growth of a multifractal structure.

IV. DISCUSSION

A number of propositions have been made to explain the origin of multifractality and multiscaling. The first is the presence of a non-Gaussian, *e.g.* power–law probability density function underlying the disorder strength η,[16]

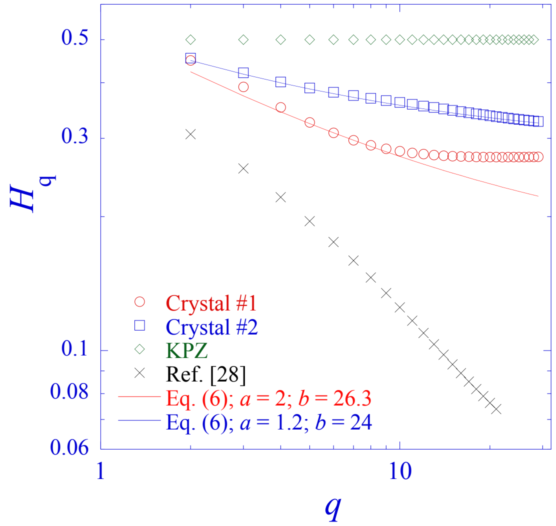

FIG. 5: The exponent H_q as a function of the order q for the magnetic flux front $Ba(Fe_{0.925}Co_{0.075})_2As_2$ crystals # 1 (○) and # 2 (□), evaluated for a given threshold of $B = 120$ G. For comparison, the (constant) H_q for the KPZ model is also shown (◇), as is the result of the analysis of the flux avalanches observed in superconducting Nb films in Ref.[28] (×). The decay of H_q measured on the superconducting samples is monotonous, without any inflection; H_q saturates at a lower, resolution–limited bound.

introduced for the description of percolative imbibition of a fluid by paper. The link between penetrating flux fronts and the porous medium equation for the imbibition by fluids was previously remarked in Refs. 1,23. However, the porous medium equation as analyzed in Ref. 23 as such does not lead to (multi–)fractal behavior.

A second explanation of anomalous scaling in roughening processes is the occurence of avalanches[15,24–27]. In particular, Bassler *et al.* explicitly showed the mutlifractal character of braided vortex trajectories in a strongly pinning superconductor[25]. The effect of a non-zero, non-constant temperature on the nucleation and propagation of dendritic vortex avalanches in thin superconducting films was described numerically, and experimentally observed in superconducting Nb by Aranson *et al.*.[28] In the problem studied by Aranson *et al.*, avalanches in defect-free films occur at periodic locations, while avalanches in films with edge defects are initiated at these imperfections. We have analyzed the structure of the flux front resulting from superposed avalanches, such as reported for the Nb films in Fig. 3 and the supplemental material (movie 8) of Ref. 28, using the correlation function (5), and find that the avalanches structure is described by a superposition of different fractal dimensions. Figure 5 shows that many orders are necessary to describe completely the set of fractal dimensions. In Aranson *et al.*'s case, the Hurst exponent starts off with a lower value < 0.5, and converges to

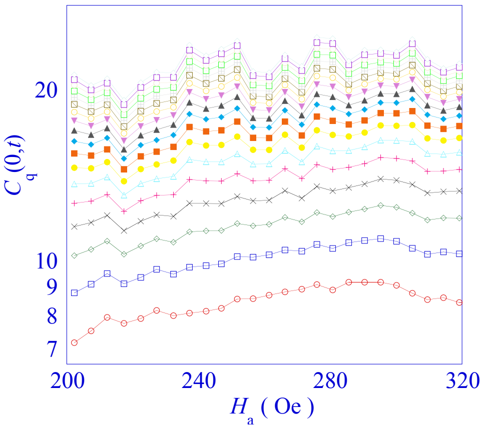

FIG. 6: Higher-order two-point correlation function as function of the temporal evolution of the magnetic flux front in $Ba(Fe_{0.925}Co_{0.075})_2As_2$ crystal # 1, at $T = 11$ K. Data are represented with the temporal variable on the abscissa expressed as the value of the externally applied magnetic field. The $C_q(0,t)$ are parallel for all q, ranging from $q =$ (bottom) to $q = 20$ (top). For the establishment of these curves, only the field values between 197 and 393 G were taken into account – for lower fields, flux does not penetrate, for higher fields, complete penetration is achieved.

zero as q increases. The avalanche–induced flux penetration of Ref. 28 also obeys multiscaling during growth, see Fig. 7. We suggest that the observed q-dependence is induced by the avalanche size distribution, which follows a power–law distribution in space and time. Clearly, the growth of the multi-fractal structures observed in the $Ba(Fe_{0.925}Co_{0.075})_2As_2$ crystals is not well described as a superposition of thermo-magnetic avalanche-like instabilities, which may explain the small difference in the generalized Hurst exponent of the roughened front.

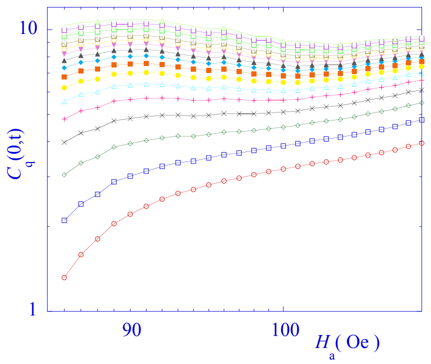

FIG. 7: Multi-scaling analysis of the growth behavior of the flux-fronts in the Nb-thin film sample of Ref. 28. Contrary to the case of $Ba(Fe_{0.925}Co_{0.075})_2As_2$, $C_q(0,t)$ has a q-dependent temporal behavior also. The q–dependent correlation function starts with a certain slope at small time, before flattening to a slope of zero at large times.

A more pertinent analogy may be that suggested by the analysis of roughened ferro-electric domain walls.[29] In that particular work, mono-affine scaling of the domain-walls, corresponding to weak collective pinning, was found on small length scales, both in numerical simulations as in actual experiments on $Pb(Zr_{0.2}Ti_{0.8})O_3$, while analysis on larger length scales showed multi-affine scaling. The crossover length scale in the study[29] was given by that on which rare events in the form of strongly pinning defects such as dislocations occur. Translated to our experiments, this would correspond to the mono-affine (KPZ-like) growth of individual front sections emanating from specific sections of the boundary of the superconducting crystal, separated by sections from which flux penetration is less likely. An interpretation of such edge inhomogeneity in terms of the local variation of superconducting properties[19] and / or geometrical irregularities at the crystal edges seems natural.

Finally, we provide a purely heuristic description of the non-trivial qq-dependence. The data in Fig. 5 are well described by

$$H_q(q) = c + \frac{a}{\sqrt{bq+1}}, \tag{6}$$

with $a = 2$ and $b = 26.3$ for crystal # 1, and $a = 1.2$ and $\beta = 24$ for crystal # 2. These values are remarkably similar to $a = 2.5$ and $b = 24$ describing the q–dependence of the exponent $\alpha(q)$ describing the metric of the harmonic measure of two–dimensional near-critical percolation clusters.[30] The harmonic measure is characterized by a lower dimension than the cluster itself, due to the inaccessibility of sites situated on deep “fjords” on the latter. There is, in fact, some similarity between such percolation clusters and the roughening and coalescence of different sections of the magnetic flux front, originating from different points of entry on the sample boundary.

Coalescence was considered in the numerical study of linear polymers on percolation clusters by Blavatskaa and Janke.[12] They proposed that multiscaling could arise from two fractal structures of different dimensions meeting each other, all the while keeping their underlying geometry[12]. Once a cluster is formed, its temporal roughening is characterized by a certain growth exponent; the cluster retains the same geometry and dimension during growth. This behavior could account for both the observed temporal monoscaling growth behavior and the multifractal roughening upon the collision of two roughened structures.

V. SUMMARY AND CONCLUSIONS

We have measured and analyzed magnetic flux-penetration fronts in single crystals of the optimally–

doped iron based superconductor $\mathrm{Ba(Fe_{0.925}Co_{0.075})_2As_2}$ superconductor, over a wide range of temperatures. Analysis of the flux fronts reveal a regular KPZ-like growth, but "anomalous" multi–fractal scaling of the two-point spatial higher–order correlation functions of the roughened flux front. Scaling does not depend on temperature, on the induction threshold used to define the front position, or on macroscopic defects that may exist in particular samples. The behavior is in agreement with multi–fractal roughening due to the aggregation of many vortex clusters with various fractal dimensions. Nevertheless, in the considered range of temperature, between 8 K and T_c, it was not possible to distinguish such clusters once a continuous flux front was formed. We suppose their existence to be due to the existence of specific sections of preferential magnetic flux penetration along the crystal edges, such as these would result from heterogeneity of the superconducting properties.[19] Once the macro cluster is formed, the front develops in time (*i.e.* in increasing magnetic field) with a classical KPZ exponent, whose university class includes DPD (directed percolation depinning).[8,9] This unusual roughening might be explained by a 2D percolation model that fits the experimental values,[30] and underscores the analogy between percolation in porous media and vortex kinetic penetration in inhomogeneous superconductors.

Acknowledgements

This work done was partially funded by the grant "MagCorPnic" of the Réseau Thématique de Recherche Avancée "Triangle de la Physique" du Plateau de Saclay, and by the Agence Nationale de la Recherche grant "PNICTIDES".

---

[1] R. Surdeanu, R. J. Wijngaarden, E. Visser, J. M. Huijbregtse, J. H. Rector, B. Dam, and R. Griessen, Phys. Rev. Lett. **83**, 2054 (1999).

[2] R. Surdeanu, R. J. Wijngaarden, B. Dam, J. Rector, R. Griessen, C. Rossel, Z. F. Ren, and J. H. Wang, Phys. Rev. B **58**, 12 467 (1998)

[3] S. He, G. L. M. K. S. Kahanda, and P-Z. Wong, Phys. Rev. Lett. **69**, 3731 (1992).

[4] J. Maunuksela, M. Myllys, O.-P. Kähkönen, J. Timonen, N. Provatas, M. J. Alava, and T. Ala-Nissila, Phys. Rev. Lett. **79**, 1515 (1997).

[5] Romualdo Pastor-Satorras, Phys. Rev. E **56**, 5284 (1997).

[6] A.-L. Barabási and H. E. Stanley, in *Fractal Concepts in Surface Growth* (Cambridge University Press, Cambridge, U.K., 1995).

[7] Mehran Kardar, Giorgio Parisi, and Yi-Cheng Zhang Phys. Rev. Lett. **56**, 889 (1986).

[8] Luís A. Nunes Amaral, Albert-László Barabási, and H. Eugene Stanley, Phys. Rev. Lett. **73**, 62 (1994).

[9] Luís A. Nunes Amaral, Albert-László Barabási, Hernán A. Makse, and H. Eugene Stanley, Phys. Rev. E **52**, 4087 (1995).

[10] Albert-László Barabási, Roch Bourbonnais, Mogens Jensen, János Kertész, Tamás Vicsek, and Yi-Cheng Zhang, Phys. Rev. A **45**, R6951 (1992).

[11] Hans-Karl Janssen, Olaf Stenull, Phys. Rev. E **75**, 020801(R) (2007).

[12] Viktoria Blavatska and Wolfhard Janke, Physics Procedia **3**, Issue 3, 1431–1435 (2010).

[13] Hans-Karl Janssen, Olaf Stenull, Phys. Rev. E **85**, 011123 (2012).

[14] Heiko Leschhorn and Lei-Han Tang, Phys. Rev. E **49**, 1238 (1994).

[15] Maya Paczuski, Sergei Maslov, and Per Bak, Phys. Rev. E **53**, 414 (1996).

[16] S.V. Buldyrev, A.-L. Barabási, F. Caserta, S. Havlin, H.E. Stanley, and T. Vicsek, Phys. Rev. A **45**, R8313 (1992).

[17] V.K. Vlasko-Vlasov, U. Welp, V. Metlushko, and G.W. Crabtree, Phys. Rev. B **69**, 140504(R) (2004).

[18] K. Ishida, Y. Nakai, and H. Hosono, *To What Extent Iron-Pnictide New Superconductors Have Been Clarified: A Progress Report* , Journal of the Phys. Society of Japan **78**, 062001(2009); David C. Johnston, *The puzzle of high temperature superconductivity in layered iron pnictides and chalcogenides* , Advances in Physics **59**, 803 (2010);

[19] S. Demirdiş, C. J. van der Beek, Y. Fasano, N. R. Cejas Bolecek, H. Pastoriza, D. Colson, and F. Rullier-Albenque, Phys. Rev. B **84**, 094517 (2011).

[20] F. Rullier-Albenque, D. Colson, A. Forget, and H. Alloul, Phys. Rev. Lett. **103**, 057001 (2009).

[21] L. A. Dorosinskĭi, M. V. Indenbom, V. I. Nikitenko, Yu.A. Ossip'yan, A. A. Polyanskii, and V. K. Vlasko-Vlasov, Physica (Amsterdam) C **203**, 149 (1992).

[22] M. Uehara, C. J. van der Beek, J. Gattacceca, V. A. Skidanov, and Y. Quesnel, Geochem. Geophys. Geosyst. **11**, Q05Y09 (2010); doi:10.1029/2009GC002653.

[23] J. Gilchrist and C.J. van der Beek, Physica (Amsterdam) C **147**, (1994).

[24] Kevin E. Bassler and Maya Paczuski, Phys. Rev. Lett. **81**, 3761 (1998).

[25] Kevin E. Bassler, Maya Paczuski, and George F. Reiter, Phys. Rev. Lett. **83**, 3956 (1999).

[26] C.M. Aegerter, R. Günther, and R.J. Wijngaarden, Phys. Rev. E **67**, 051306 (2003).

[27] C. M. Aegerter, K. A. Lörincz, M. S. Welling, and R. J. Wijngaarden, Phys. Rev. Lett. **92**, 058702 (2004).

[28] Igor S. Aranson, A. Gurevich, Marco S. Welling, Rinke J. Wijngaarden, Vitalli K. Vlasko-Vlasov, Valerii M. Vinokur, Ulrich Welp, Phys. Rev. Lett. **94**, 037002, 2005

[29] J. Guyonnet, E. Agoritsas, S. Bustingorry, T. Giamarchi, P. Paruch, arXiv:1205.0155v1 [cond-mat.mtrl-sci] (2012).

[30] B. Duplantier, Phys. Rev. Lett. **82**, 880 (1999).